

# MeV Mott Polarimetry at Jefferson Lab

M. Steigerwald

*Jefferson Lab, Newport News, Virginia 23606*

**Abstract.** In the recent past, Mott polarimetry has been employed only at low electron beam energies ( $\approx 100$  keV). Shortly after J. Sromicki demonstrated the first Mott scattering experiment on lead foils at 14 MeV (MAMI, 1994), a high energy Mott scattering polarimeter was developed at Thomas Jefferson National Accelerator Facility (5 MeV, 1995). An instrumental precision of 0.5 % was achieved due to dramatic improvement in eliminating the background signal by means of collimation, shielding, time of flight and coincidence methods. Measurements for gold targets between  $0.05 \mu\text{m}$  and  $5 \mu\text{m}$  for electron energies between 2 and 8 MeV are presented. A model was developed to explain the depolarization effects in the target foils due to double scattering. The instrumental helicity correlated asymmetries were measured to smaller than 0.1 %.

## INTRODUCTION

A Mott - polarimeter has been developed to measure the spin polarization of the electron beams produced by the sources of polarized electrons in the injector of Thomas Jefferson National Accelerator Facility. The polarimeter uses the counting rate asymmetry in the single elastic Mott scattering process which exists if the polarization vector is not parallel to the scattering plane. The Sherman - function determines the relation between measured asymmetry and the degree of polarization of the electron beam. Accurate polarimetry is ensured by addressing three concerns: First, the determination of the theoretical Sherman - function for the single elastic scattering process. Second, the correct measurement of the asymmetry for every target by the achievement of pure energy spectra and third, the understanding of the foil - thickness extrapolation to target thickness zero.

## THE POLARIMETER SETUP

The present setup of the MeV polarimeter is shown in figure 1. Early versions of the polarimeter have been described in [1]. Since the kinetic energy of the electron beam is low between 2 and 8 MeV, the polarimeter uses a vacuum vessel to enclose the scattering target avoiding any spread of the electron beam in air

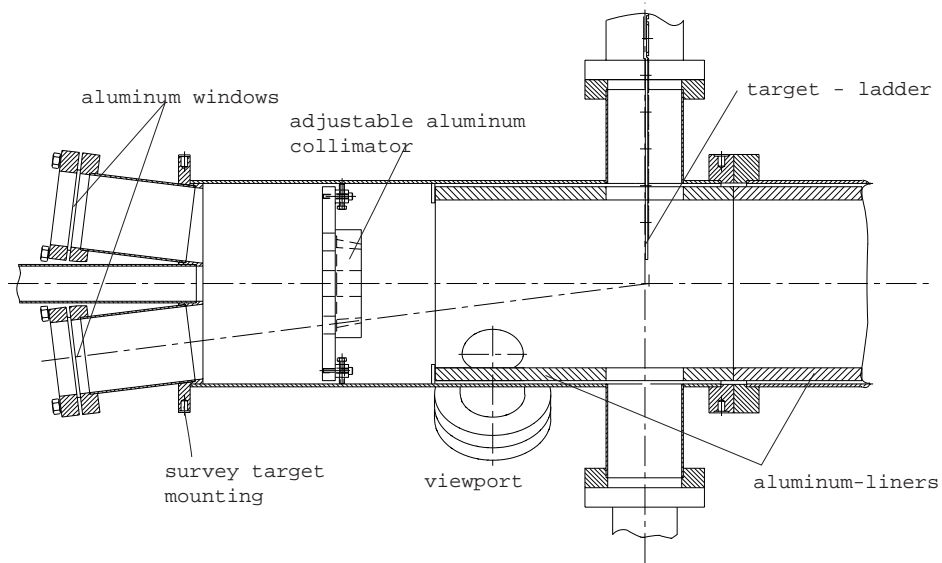


**FIGURE 1.** Cross section through the MeV Mott - polarimeter

(Fig. 1). The polarimeter's stainless steel chamber is directly connected to the vacuum beam line and can be isolated by means of a full metal valve. The electron beam is guided to the polarimeter target by a 12.5 degree dipole bend magnet, which is energized during a polarization measurement. The electrons enter the chamber from the left side of Figure 1 and hit the center of the target with a precision of 0.5 mm and an angle of less than 2 mrad. The beam spot may be observed by means of a CCD camera mounted to a side view port. It detects the transition radiation produced by the the electrons when they pass the target foil. The target ladder is mounted on a 600 mm linear drive that allows the selection of seventeen different targets. The target ladder holds 10 gold, 2 copper and 3 silver as well as a Cromox viewer and an empty target. The gold targets cover a thickness range of 500 Å to 5 μm. The polarimeter chamber has 4 ports that each support a 0.05 mm thin aluminum window, a detector assembly, and a lead collimator. Together with an additional adjustable aluminum collimator inside the vacuum chamber this arrangement defines a scattering angle of 172.6 degrees and a solid angle of 0.18 msr. The collimators are chosen to accept only scattered electrons from a foil area that has a diameter of 3 mm. The scattered electrons penetrate the aluminum windows and reach the detectors. The main electron beam is dumped into a 21 mm thick aluminum plate which serves as the end flange of a 2500 mm long, 200 mm diameter aluminum tube connected directly to the polarimeter chamber. Aluminum liners are used to minimize photon production from electrons that hit the chamber walls after scattering from the target. In order to eliminate the Bremstrahlung photons which are produced by all types of electron

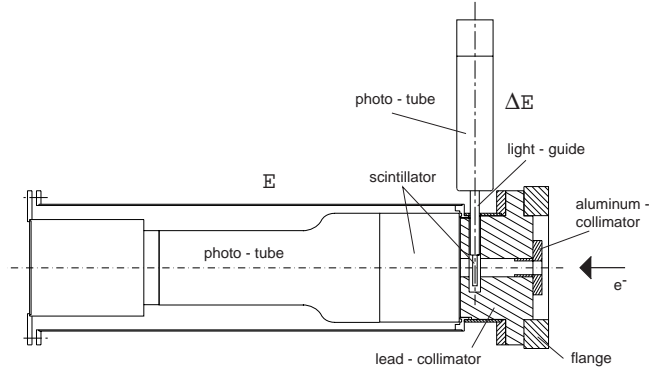


**FIGURE 2.** Cross - section of the detector arrangement

loss and field emission from nearby cryomodules a 50 to 100 mm lead shielding was constructed around the detector area.

### *Coincidence and time of flight methods*

The analyzing power is only known for single elastic scattering, so it is necessary to separate the elastic scattered electrons from the inelastics. Hence, every detector assembly possesses two scintillator / photomultiplier assemblies (fig.2). The E detector serves as a stop detector and achieves an energy resolution of about 8 %. The phototube has an active cathode area of 75 mm. A cylindrical scintillator, 75 mm long with 75 mm diameter is glued directly to the photomultiplier window. Since the photon background crosses into the elastic electron peak of the detectors energy spectra and because it is impossible to shield against the photon background generated by the dump it was necessary to install a second detector assembly  $\Delta E$  in front of the of the E detector assembly. The two detectors are run in coincidence. The  $\Delta E$  detector assembly consists out of a 2 mm thin plastic plate and a 25 mm diameter phototube. A photon producing a signal is unlikely, so the  $\Delta E$  detector serves only as a trigger. Finally, a time of flight methode was introduced in addition to the above described methodes. Instead of illuminating the photemission gun with a laser pulse rate of 500 MHz which is the standard running mode the frequency is divided by four so that the electron bunchers possess a time gap of 8 ns. Hence, the electrons that are reflected at the aluminum dump that is 6 ns away from the target may be seperated from those that are scattered at the target by triggering on the laser frequency.

Figure 3 indicates the improvement made by using the different methodes. By cleaning up the spectra so dramatically a background subtraction is not necessary any more and therefore is the asymmetry measurement precision for one foil thickness limited to the statistical errorbar.

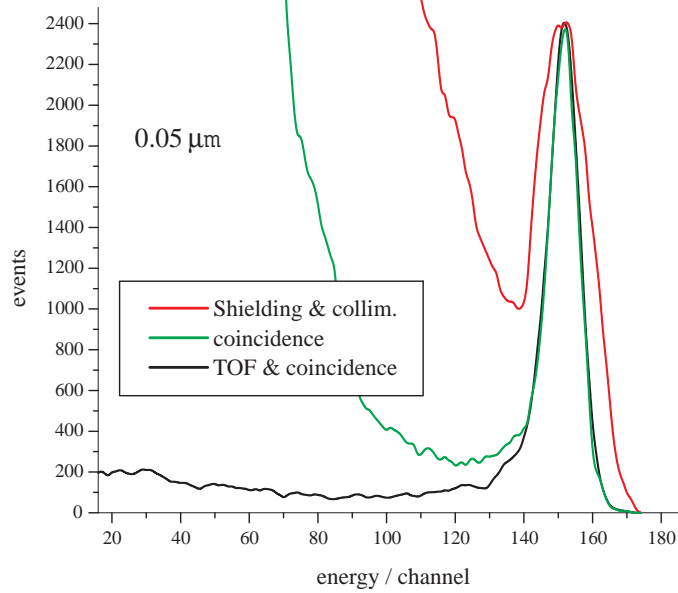


**FIGURE 3.** Energy spectra measured by means of the E detector

## ANALYZING POWER

The measured asymmetry is smaller for the thicker foil due to double scattering in the target foil. Therefore a foil thickness extrapolation has to be done to find the asymmetry for foil thickness zero that corresponds to the single elastic scattering process. In the past it was not clear which extrapolation function had to be used. This paragraph describes the calculation of the analyzing power for the single elastic scattering process as well as a new model that describes the dilution of the analyzing power with increasing foil thickness.

### *Single elastic scattering process*

The analyzing power  $S(\alpha)$  may be derived by solving the Dirac equation for a pure Coulomb potential [3] and by calculating the phase shifts of the scattering phases caused by the finite thickness of the nucleus [6]. Also important are the spin rotation functions  $T(\alpha)$ ,  $U(\alpha)$  as well as the cross section  $\sigma(\alpha)$ . These values are generously generated by Prof. Ch. Horowitz (Univ. of Indiana). They are defined by the scattering amplitudes  $f$  and  $g$ :

$$\sigma(\alpha) = |f|^2 + |g|^2 \quad S(\alpha) = i \frac{fg^* - f^*g}{|f|^2 + |g|^2} \quad T(\alpha) = \frac{|f|^2 - |g|^2}{|f|^2 + |g|^2} \quad U(\alpha) = \frac{fg^* + f^*g}{|f|^2 + |g|^2}$$

The function  $f$  and  $g$  may be found in the literature [3] [5]. The screening of the Coulomb potential by the shell electrons is not taken into account in Horowitz's

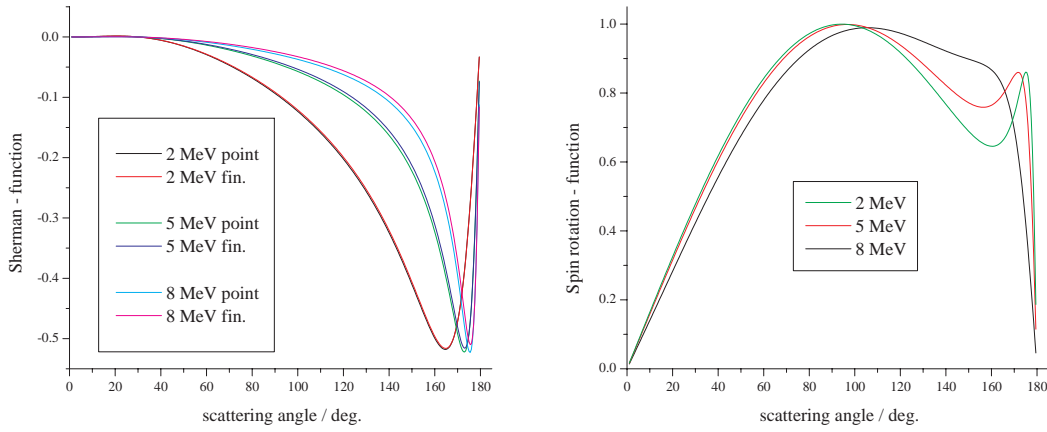


**FIGURE 4.** Sherman function and spin rotation function for 2,5 and 8 MeV

calculation as well as the recoil of the center of mass and the charge distribution of the nucleus. The dominating uncertainty is caused by radiative corrections and is estimated to be lower than 1%. Figures 4 show the results of the analyzing power and the spin rotation function for three different energies. Both solutions for point and finite size nucleus are indicated.

### *Double scattering*

In order to explain the dilution of the asymmetry in target foils of finite thicknesses a model has been developed that follows Wegeners [4] exposition, but has been done numerically. In the following the number of big angle double and small angle multiple scattered electrons will be determined. The double scattering is calculated using cross - sections  $\sigma(\alpha)$ , Sherman functions  $S(\alpha)$  and spin rotation functions  $T(\alpha)$  and  $U(\alpha)$  described in the upper section. The likelihood for triple scattering is neglected since it is very low at high electron energies in the MeV region. Hence, the following integral has to be determined

$$N = \int_{\theta=0}^{\pi} \int_{\varphi=0}^{2\pi} \int_{x_1=0}^D \int_{\vartheta=\theta_2}^{\theta_2+\Omega_\theta} 1(x_1, \theta, \varphi) \cdot 2(x_2, \theta_2) \cdot E(x_1, x_2) \quad d\vartheta \, dl \, d\varphi \, d\theta$$

The dependencies on energy and number of protons in the nucleus is not indicated. The integration has to be carried out over the whole volume of the foil. Here  $\theta$  and  $\phi$  symbolize the polar - and azimuthal - angle of the first scattering and  $dl$  an integration step in foilthickness  $D$ .  $x_1$  stands for the path between foil entrance and the first scattering, while  $x_2$  symbolizes the path after the first scattering and exit of the foil.  $1(x_1, \theta, \varphi)$ ,  $2(x_2, \theta_2)$  describe the first and second scattering processes,

while  $E(x_1, x_2)$  contains the impulse height spectra.  $E(x_1, x_2)$  is achieved by Monte Carlo simulations and has different characteristics for foil thickness, the distances in the foil  $x_1$  and  $x_2$  and Energy and includes electron loss between the first and second scattering and electron absorption in the target. Therefore, it compensates the singularity that arises for scattering under 90 degrees when the electron travels parallel to the target surface and  $x_2$  becomes infinit. The fourth integral is executed because of the change of  $2(x_2, \theta_2)$  over the detector acceptance. The first scattering may be written as

$$1(x_1, \theta, \varphi) = I \cdot \frac{A_v \rho}{A} \cdot \sigma_1(\theta) \cdot x_1 \cdot \Omega_\varphi \cdot (1 + S(\theta_1) \cdot \vec{P}_i \hat{n}_1)$$

$I$  is the incident electron current,  $A_v$  the Avogadro number,  $\rho$  the density of the target material,  $x_1$  the path in the foil and  $\Omega_\varphi$  the detector acceptance. The singularity of the modified Mott cross - section at a small angle is solved by means of GEANT simulations. Cross - sections for angles lower than the critical Møller angle are substituted by the results of the Monte Carlo simulation, which represents multiple scattering. The residual polarization after the first scattering is:

$$\vec{P}^\dagger = \frac{(\vec{P}_i \hat{n}_1 + S(\alpha)) \cdot \hat{n}_1 + T(\alpha) \cdot \hat{n}_1 \times (\vec{P}_i \times \hat{n}_1) + U(\alpha) (\hat{n}_1 \times \vec{P}_i)}{1 + \vec{P}_i \hat{n}_1 S(\alpha)}$$

The second scattering for the up ( $u$ ) and down ( $d$ ) detector results to

$$2(x_2, \theta_2)_{ud} = x_2 \cdot (1 + S(\theta_{2,ud}) \cdot \vec{P}^\dagger \hat{n}_{2,ud}) \cdot \sigma(\theta_{2,ud})$$

where  $\theta_2$  is the angle of the second scattering. The dependency of the cross section of the second scattering on the energy loss between first and second scattering is also taken into account.

## *Result*

Figure 5 shows the number of electrons that hit the up and down detectors as a function of the first scattering angle  $\theta_1$ . The numbers are calculated for an incident beam of  $1 \mu A$  and with an energy of 5 MeV having transverse polarization of 100 %. The target is a  $5 \mu m$  gold - foil. The 0 to 20 (160 to 180) degree peaks may be described as electrons that have a scattering with a first (second) small angle and a large second (first) scattering that possesses a high analyzing power. That produces a counting rate asymmetry between up and down detector. The peak at 90 degrees exists because the path  $x_2$ , and therefore the scattering probability  $2(x_2, \theta_2)_{ud}$ , becomes large. The integration over  $\phi$  and the Sherman function of 4.3 % at 90 degrees lead to a small counting rate asymmetry between the up and down detectors. Writing the counting rate for up and down detector as the sum of polarization dependend portion  $A$  and independend portion  $U$

$$N_{ud} = (1 \pm PS) \cdot A + U$$

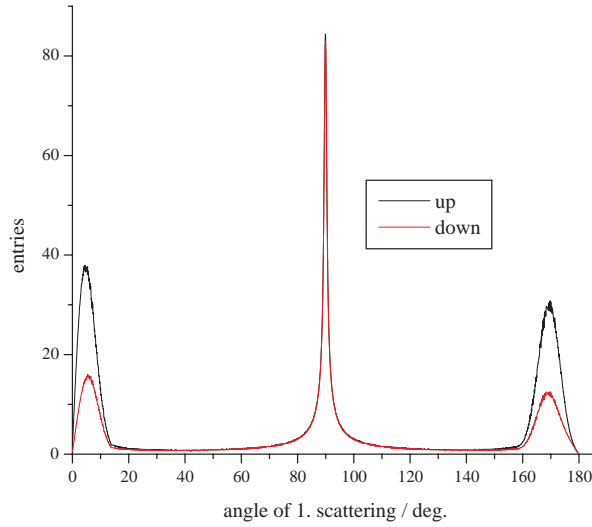


**FIGURE 5.** The polarization of the incident electrons is perpendicular to the scattering plane and its degree is 1. Number of electrons in the up and down detector in dependency of the first scattering angle

It follows the analyzing power in dependency of the foil thickness:

$$S(d) = S(0) \frac{1 + 0.00272d^{0.866}}{1 + 0.23d^{0.866} + 0.0729d + 0.0146d^2 + 0.00339d^3}$$

The upper result is only correct if an energy cut is made at the center of the elastic peak. This is because the polarization dependent and independent portions have varying energy losses in the target material and have therefore different energy spectra.

## CALIBRATION

Figure 6 compares the measurement (points with error bars) of foil thickness extrapolations for three different energies and the corresponding calculations (lines). The only free parameter in each case was the degree of spin polarization. Since the energy measurement results in an uncertainty of relative 0.3 % and each extrapolation to a statistical variance of 0.3 % all three extrapolations agree within the error bars. That leads to the conclusion that not only the form of the extrapolation function is understood but also that the calculation for the analyzing power agrees relatively well with each other. All investigations lead to the following result: The uncertainty of the extrapolated asymmetry at foil thickness zero is smaller than 0.5 %. The analyzing power for the single elastic scattering process is known to a

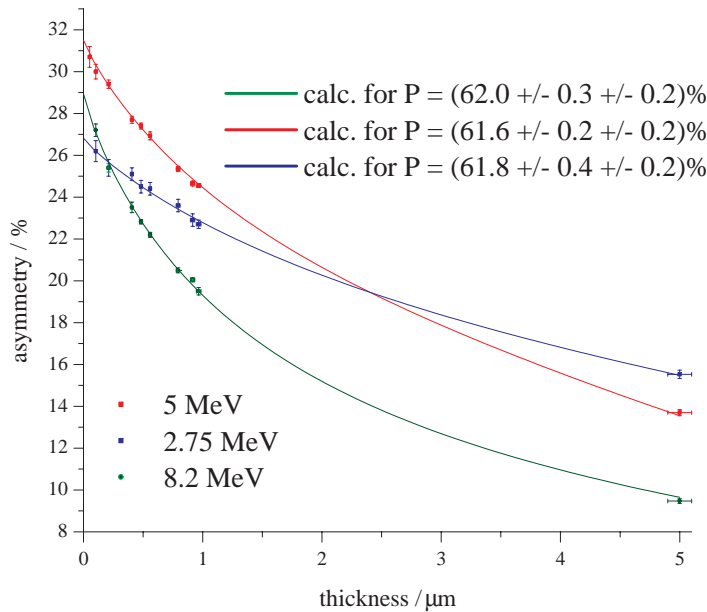


**FIGURE 6.** Foil - thickness extrapolation for 2.75, 5 and 8.2 MeV. Lines symbolize calculation and dots the measurement.

precision of 1%. This results in a systematic uncertainty of the polarization measurement process of 1.1%.

The instrumental asymmetry was determined to  $(4 \pm 6) \cdot 10^{-4}$  by using an unpolarized electron beam. The asymmetries in both polarimeter arms agree within the statistical error bars. No significant dependency of the asymmetry was observed by varying the electron position on the target foil in an area of 10 mm diameter.

## ACKNOWLEDGEMENT

This work was supported by the USDOE under contract DE-AC05-84ER40150. Special thanks to A. Day and B. Wojtsekhowski for their continuous support.

## REFERENCES

1. Price, J.S., *Proceedings of 13th International Symposium High Energy Spin Physics*, 554 (1998).
2. Sromicki, J., *Phys. Rev. Let.* **81**(1), 57 (1999).
3. Sherman, N., *Phys. Rev.* **103**(6), 1601 (1956).
4. Wegener, H., *Zeitschrift f. Physik* **151**, 252 (1958).
5. Mott, N.F., Massey, H.S.W., *Theory of Atomic Collision*, Oxford: Clarendon Press, 1965, ch. 6, pp. 23-26.
6. Horowitz, Ch. Private communication, (2000).